

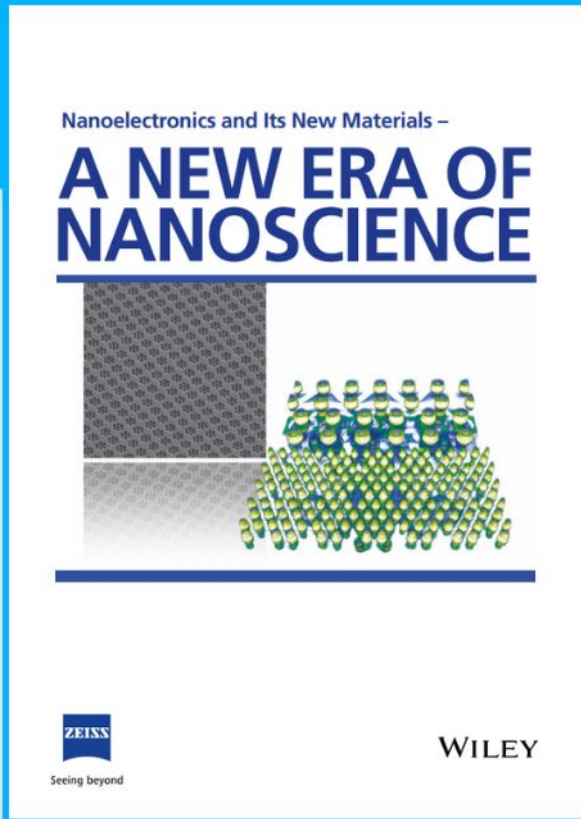


Nanoelectronics and Its New Materials – A NEW ERA OF NANOSCIENCE

Discover the recent advances in electronics research and fundamental nanoscience.

Nanotechnology has become the driving force behind breakthroughs in engineering, materials science, physics, chemistry, and biological sciences. In this compendium, we delve into a wide range of novel applications that highlight recent advances in electronics research and fundamental nanoscience. From surface analysis and defect detection to tailored optical functionality and transparent nanowire electrodes, this eBook covers key topics that will revolutionize the future of electronics.

To get your hands on this valuable resource and unleash the power of nanotechnology, simply download the eBook now. Stay ahead of the curve and embrace the future of electronics with nanoscience as your guide.



Seeing beyond

WILEY

Sulfur Promotion in Au/C Catalyzed Acetylene Hydrochlorination

Simon R. Dawson, Samuel Pattisson, Grazia Malta, Nicholas F. Dummer, Louise R. Smith, Anna Lazaridou, Christopher S. Allen, Thomas E. Davies, Simon J. Freakley, Simon A. Kondrat, Christopher J. Kiely, Peter Johnston, and Graham J. Hutchings*

The formation of highly active and stable acetylene hydrochlorination catalysts is of great industrial importance. The successful replacement of the highly toxic mercuric chloride catalyst with gold has led to a flurry of research in this area. One key aspect, which led to the commercialization of the gold catalyst is the use of thiosulphate as a stabilizing ligand. This study investigates the use of a range of sulfur containing compounds as promoters for production of highly active Au/C catalysts. Promotion is observed across a range of metal sulfates, non-metal sulfates, and sulfuric acid treatments. This observed enhancement can be optimized by careful consideration of either pre- or post-treatments, concentration of dopants used, and modification of washing steps. Pre-treatment of the carbon support with sulfuric acid (0.76 M) resulted in the most active Au/C in this series with an acetylene conversion of $\approx 70\%$ at 200°C .

The addition of a second metal has demonstrated various improvements such as stabilizing Au active species by preventing reduction of Au (I) or Au (III),^[3–7] increasing electron density of active species, and thereby promoting chemisorption of HCl which inhibits reduction of the gold,^[8–11] promoting a higher dispersion of the gold,^[12,13] and decreasing the formation of nanoparticles by agglomeration.^[14] However, the addition of another metal can also incur drawbacks such as lower selectivity, which can lead to coke deposition and rapid deactivation of the catalyst,^[13] short lifetime of the catalyst,^[3,15] or the requirement of high loadings of the second metal to achieve com-

parable results to the gold monometallic.^[5,13,16] In addition to these issues, a secondary metal may also lead to complications with precious metal recovery from spent catalysts.^[17,18] Therefore non-metallic promoters are an interesting alternative for enhancing the activity and stability of gold catalysts for acetylene hydrochlorination. Zhang et al. investigated the modification of gold catalysts with nitrogen, phosphorous, and oxygen containing ligands. The authors concluded that coordination with these heteroatoms stabilized cationic gold species due to increased electron density around the active species. This also promoted a higher surface concentration of HCl compared with acetylene which facilitates the hydrochlorination

1. Introduction

The production of vinyl chloride monomer (VCM) from the hydrochlorination of acetylene is an important industrial process which continues to increase in scale. The replacement of the highly toxic mercuric chloride catalyst for this process represented a major environmental landmark, brought about by the signing of the Minamata convention.^[1] The commercialization of a carbon supported gold catalyst has led to an increased focus in this area to produce highly active and stable materials.^[2]

Various studies have reported the use of bimetallic catalysts and dopants for the improvement of these characteristics.

Dr. S. R. Dawson, Dr. S. Pattisson, Dr. G. Malta, Dr. N. F. Dummer, L. R. Smith, A. Lazaridou, Dr T. E. Davies, Prof. G. J. Hutchings
Cardiff Catalysis Institute
School of Chemistry
Cardiff University
Main Building, Park Place, Cardiff CF103 AT, UK
E-mail: Hutch@cf.ac.uk
Dr. C. S. Allen
Department of Materials
University of Oxford
Oxford OX1 3PH, UK

Dr. C. S. Allen
Electron Physical Sciences Imaging Centre
Diamond Light Source Ltd.
Oxfordshire OX11 0DE, UK
Dr. S. J. Freakley
Department of Chemistry
University of Bath
Bath BA2 7AX, UK
Dr. S. A. Kondrat
Department of Chemistry
Loughborough University
Loughborough LE11 3TU, UK
Dr. C. J. Kiely
Department of Materials Science and Engineering
Lehigh University
Bethlehem, PA 18015, USA
Dr. P. Johnston
Process Technologies
Johnson Matthey
Billingham TS23 1LB, UK

 The ORCID identification number(s) for the author(s) of this article can be found under <https://doi.org/10.1002/smll.202007221>.

© 2021 The Authors. Small published by Wiley-VCH GmbH. This is an open access article under the terms of the Creative Commons Attribution License, which permits use, distribution and reproduction in any medium, provided the original work is properly cited.

DOI: 10.1002/smll.202007221

reaction.^[19] Nitrogen has also successfully been used to dope metal-free carbon catalysts resulting in increased acetylene conversion.^[20–22] The activity of N-doped carbons has been further enhanced by introducing sulfur via a sulfuric acid treatment.^[23] The increased activity was attributed to an increased adsorption of acetylene. Di et al. demonstrated the beneficial use of thiourea as an additive to carbon supported gold catalysts.^[24] It was suggested that sulfur serves as an anchor for gold which prevents reduction of the active species. Qi et al. demonstrated the successful use of a sulfur containing ionic liquid, trimethylsulfonium iodide, in the preparation of Au/C catalysts.^[25] The enhanced activity was ascribed to increased adsorption of the reactants, in particular HCl, and desorption of the VCM product. The role of sulfur moieties in carbon supported gold catalysts for this reaction has been studied in detail by Duan et al.^[26] The team demonstrated that high valency sulfur species such as $-\text{SO}_3\text{H}$ and $-\text{SO}_2\text{H}$ stabilized the cationic nature of gold nanoclusters, enabling high activity and stability, whereas low valence type molecules such as $-\text{SH}$ destabilize cationic gold leading to agglomeration and deactivation.

Sulfur has played an important role in the industrial viability of the gold catalysts. Initial supported single-atom catalysts prepared from aqua regia deposition of chloroauric acid were not considered viable due to short lifetimes resulting from nanoparticle formation. Furthermore, there are difficulties associated with large scale production. Johnston and co-workers reported the effectiveness of soft donor ligands such as thiosulphate, as a method to improve the stability of the supported gold by maintaining oxidized species.^[2] Our group recently confirmed the presence of a redox couple comprised of Au(I) and Au(III) to be responsible for the activity observed.^[27] This, coupled with the improved ease of production compared to previous preparative methods with aqua regia, has led to the successful commercialization of a carbon supported gold-thiosulfate catalyst. Previous work in our group has highlighted the importance of oxidation state of the gold, choice of solvent, and more recently the nature of S and Cl ligand environment for formation of stable gold catalysts.^[28] This study examines the use of various sulfur containing compounds and preparation methods for the enhancement in activity of Au/C acetylene hydrochlorination catalysts.

2. Results and Discussion

2.1. Doping Au/C with Transition Metal Sulfates

Initially, three metal sulfates were investigated for their effect as dopants and compared to the standard aqua regia catalyst (Au/C-AR). Catalysts were prepared by stirring the carbon support in saturated aqueous solutions of cobalt, manganese, and iron sulfate in order to achieve a high loading of each dopant, followed by washing and drying. Finally, gold was deposited onto the doped carbon from a solution of chloroauric acid dissolved in aqua regia. The choice of cobalt sulfate was due to previous reports that cobalt has been shown to enhance the activity of gold catalysts in this reaction.^[3,8] It was suggested that the inclusion of cobalt increases the relative concentration of Au(I) and Au(III) species, reduces sintering, and inhibits coke deposition. Manganese and iron were chosen as neighboring transition metals for comparison. Each of the prepared catalysts were tested for the acetylene hydrochlorination reaction, and the maximum conversion during the test period (240 min) is illustrated in **Figure 1a**. Both the Au/C- CoSO_4 and Au/C- MnSO_4 catalysts exhibited much higher activity (47% and 37% acetylene conversion, respectively) than that over monometallic Au/C-AR (19%). However, Au/C- FeSO_4 maintained a low conversion throughout the test (5%). The low activity of the gold free Co and Mn doped carbons (4% and 3% respectively) suggests that the enhanced activity in the presence of gold is due to a synergistic effect and not simply a summation of the parts. Powder X-ray diffraction (XRD) exhibited no reflections arising from gold or other metals suggesting no nanoparticles were present in any of the fresh samples, with only two broad reflections for carbon being observed at 24° and $44^\circ/2\theta$ (Figure S1, Supporting Information). The Au/C- FeSO_4 sample was the only one to contain reflections characteristic of gold nanoparticles in the used sample, suggesting agglomeration had occurred during the reaction. It is possible that the low activity of this sample is due to Au agglomeration during the pre-heating of the catalyst to 200°C , or immediately upon introduction of the reactant gases. The low activity may also be explained by the significantly higher concentration of a second metal and sulfur in the Au/C- FeSO_4 sample compared to the other prepared catalysts as confirmed by X-ray photoelectron spectroscopy (XPS) (Table S1, Supporting Information). Such a high concentration

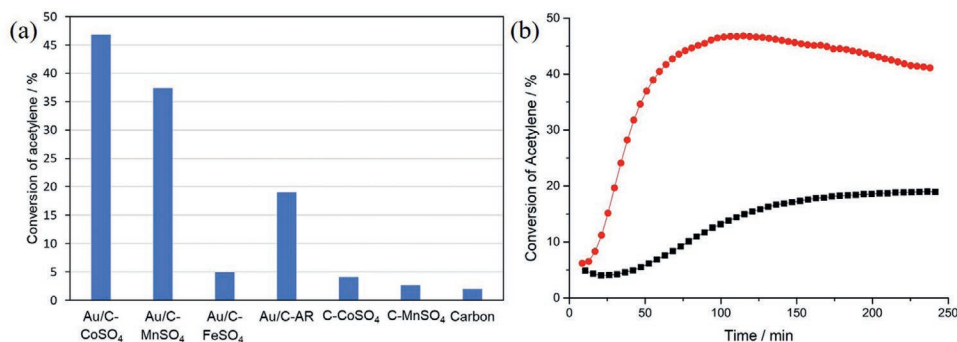


Figure 1. a) Comparison of acetylene conversions for Au/C- CoSO_4 , Au/C- MnSO_4 , and Au/C- FeSO_4 catalysts and their respective treated carbons. b) Au/C- CoSO_4 time-on-line data—Au/C- CoSO_4 (●), Au/C-AR (■).

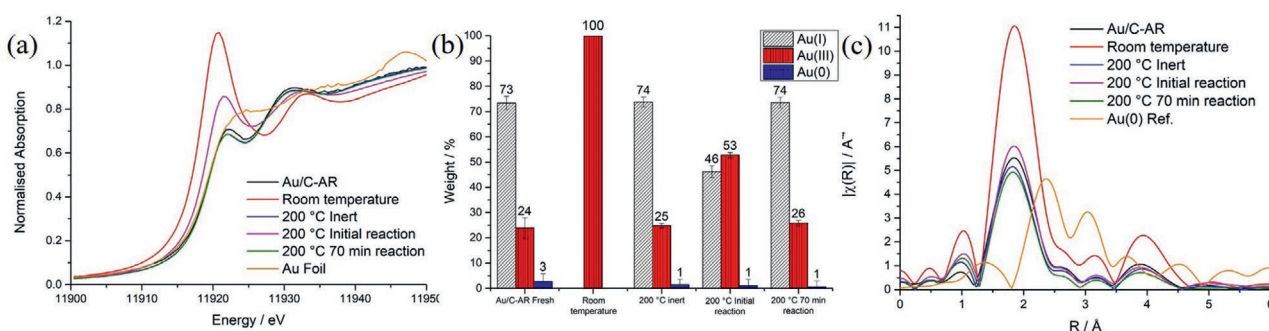


Figure 2. a) Au L₃-edge XANES of Au/C-AR, Au/C-CoSO₄ at room temperature, after heating to 200 °C under inert conditions, after introduction of reaction gases at 200 °C, and after 70 min of reaction and Au foil reference. Note that the data for 200 °C Inert (blue line) is nearly identical to and therefore hidden by the data 200 °C 100 min reaction (green line). b) Linear combination fitting of the Au L₃-edge XANES for Au/C-AR, Au/C-CoSO₄ at room temperature, after heating to 200 °C under inert conditions, after introduction of reaction gases at 200 °C, and after 70 min of reaction and Au foil reference. c) Fourier transform of the k₃-weighted χ EXAFS data of Au/C-AR, Au/C-CoSO₄ at room temperature, after heating to 200 °C under inert conditions, after introduction of reaction gases at 200 °C, and after 70 min of reaction and Au foil reference.

may poison the active species while also having a detrimental effect on the stability of the atomically dispersed gold.

The reaction activity as a function of time-on-line for the most active catalyst, Au/C-CoSO₄, displays a similar induction period to the standard Au/C-AR catalyst (Figure 1b). However, the acetylene conversion reaches a maximum conversion of 47% after 100 min compared to a maximum of ≈20% conversion in Au/C-AR. This higher conversion is accompanied by a modest deactivation which is not observed in Au/C-AR over the same testing period. X-ray absorption spectroscopy (XAS) was performed to compare gold oxidation state in that of the Au/C-CoSO₄ and Au/C-AR, and to monitor any potential changes in S and Cl ligation (Figure 2). In situ gold L₃-edge X-ray absorption near edge structure (XANES) was performed to monitor changes in the gold oxidation state of Au/C-CoSO₄ before and during the reaction (Figure 2a). Initially, the supported Au was present solely as Au(III), as noted by a large white line height. When heated to 200 °C under a He atmosphere, the absorption intensity decreased, signifying more Au(I) content, very similar to that of the fresh Au/C-AR. Introduction of the reaction gases caused a rapid oxidation to a more Au(III) like state, which was reduced to Au(I) over the course of the 70 min induction period. This is supported by previous work, suggesting that Au(I) is conducive to high acetylene conversion.

A linear combination fitting (LCF) of the XAS results was performed (Figure 2b) to quantify the proportions of gold oxidation states during the analysis, with reference to the Au(I) and Au(III) standards (Figure S2, Supporting Information). This confirmed that the initial state of the catalyst at room temperature is exclusively Au(III), with no fractions of other oxidation states present. Heating to 200 °C under inert conditions reduced the Au significantly to Au(I)—74% and Au(III)—25%. These fractions of Au were remarkably similar to those of Au/C-AR (Au(I)—78%, Au(III)—19%, and Au(0)—3%). Introduction of the reaction gases caused oxidation of gold, to Au(III)—53%, leaving the remainder as Au(I)—46%. However, after 70 min of reaction the gold again partially re-oxidized, Au(I)—74% and Au(III)—26%, to a state similar to that of Au/C-AR under reaction conditions. In each of the reaction stages, a small percentage of Au(0) is also reported, however in all cases this is within the error of the analysis and

considered negligible. Analysis by extended X-ray absorption fine structure (EXAFS) determined the short-range order of the catalysts at the different stages of the reaction (Figure 2c). In all cases, the catalyst showed a distinct scattering peak at 1.8 Å corresponding to Au—Cl, although the intensity of this was significantly higher in Au/C-CoSO₄ at room temperature compared to Au/C-AR. All XAS measurements were taken during in situ experiments, therefore under identical conditions, which suggests a genuinely greater concentration of Au—Cl or Au—S, both indistinguishable via EXAFS.^[27] However, after heating this intensity reduced to a comparable level to that of Au/C-AR, indicating a change in oxidation state. No reflections at 2.5 and 3.0 Å were detected, suggesting no significant Au nanoparticle formation under reaction conditions which is in agreement with the data obtained from XANES and XRD. This analysis demonstrated that the addition of CoSO₄ to the carbon support prior to Au deposition, increased the initial acetylene conversion, by oxidizing the Au species present before reaction to Au(III). This increased the rate at which the gold reduced to the active Au(I) species, as observed in the Au/C-AR catalyst. However, this increased activity is accompanied with a deactivation profile not observed in Au/C-AR or indeed the commercial thiosulfate catalysts.

2.2. Doping Au/C with Non-Transition Metal and Non-Metal Sulfates

Sodium sulfate and ammonium sulfate were chosen to replace the above transition metal sulfates to further elucidate the effect of sulfate on the catalytic performance and denoted “pre-wash” catalysts. In addition, a “post-wash” catalyst was prepared whereby the prepared Au/C-AR catalyst was stirred in the salt sulfate solution, followed by filtering, washing, and drying. Finally, a third catalyst was prepared using the salt sulfate solution instead of aqua regia referred to as “no-AR”.

The catalysts prepared with (NH₄)₂SO₄ were tested for the acetylene hydrochlorination reaction (Figure 3a). (NH₄)₂SO₄ pre-wash showed a much higher conversion (45%) than that over Au/C-AR (18%) albeit with a similar reaction profile; an induction period lasting roughly 240 min before stabilizing at

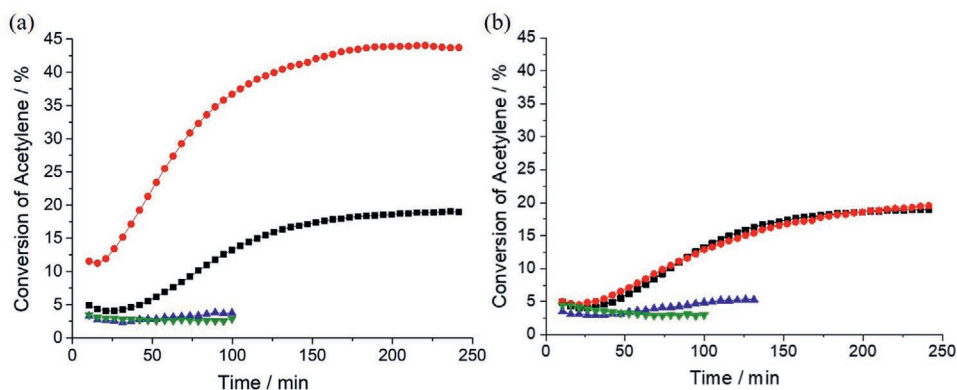


Figure 3. a) Comparison of acetylene conversion over time for a series of $(\text{NH}_4)_2\text{SO}_4$ treated catalysts; b) comparison of acetylene conversion over time for a series of Na_2SO_4 treated catalysts time-on-line data—pre-wash (●), post-wash (▲), no AR (▼), and Au/C-AR (■).

a constant conversion. This suggests that sulfate is responsible for the increase in catalyst activity, as opposed to the metals introduced in the previous section. Both $(\text{NH}_4)_2\text{SO}_4$ post-wash and no-AR catalysts exhibited poor conversion (3%), comparable to that over the carbon control (2%). XRD analysis of the three fresh catalysts determined that both $(\text{NH}_4)_2\text{SO}_4$ post-wash and no-AR catalysts contained nanoparticles prior to reaction (Figure S3a, Supporting Information), whilst the pre-wash displayed no gold reflections. This result was not unexpected for the no-AR sample as water is known to be a poor solvent for preparation of Au/C catalysts from HAuCl_4 due to its low oxidizing ability.^[27,29] This leads to reduction of the gold and formation of inactive nanoparticles. XRD of a post-wash preparation using a fresh Au/C-AR catalyst and water, instead of the $(\text{NH}_4)_2\text{SO}_4$ solution confirmed that the additional water, combined with drying at 110 °C mobilized the gold on the surface of the support leading to agglomeration and formation of nanoparticles (Figure S3b, Supporting Information).

Reactions were performed on a similar trio of catalysts prepared with Na_2SO_4 (pre-wash, post-wash, and no-AR) (Figure 3b). Here, the pre-wash of Na_2SO_4 had no effect on the catalytic performance with an almost identical reaction profile to that of Au/C-AR. Poor conversion was recorded over both the post-wash (conversion of 5%) and no AR catalysts, with the latter deactivating in the short reaction time from 5% to 3%. XRD analyses of this catalyst series were similar to those where $(\text{NH}_4)_2\text{SO}_4$ was used and where no nanoparticles were observed in the pre-wash catalyst, but large reflections were observed in both the post-wash and no-AR catalysts (Figure S4, Supporting Information). These results demonstrate that it is possible to produce highly active catalysts without the presence of another metal, merely with the addition of the sulfate anion. However, this enhancement is seemingly sensitive to the choice of cation, the extent of doping and the order in which it is applied to the support.

2.3. Sulfuric Acid Treated Catalyst

Due to the observed enhancement with non-metal sulfates, we treated the carbon support with sulfuric acid. Carbon was treated using the same preparations as mentioned previously with sulfuric acid; “pre-wash”, “post-wash”, and “no-AR”.

2.3.1. Pre-Treatment of Carbon Supports with Sulfuric Acid

Carbon was stirred in three dilute solutions (0.076, 0.76, and 1.52 M) of sulfuric acid to form pre-wash carbons. Gold was then deposited on these supports using aqua regia. Subsequently, the samples were tested for the acetylene hydrochlorination reaction and time-on-line data for obtained (Figure 4). All three catalysts displayed far higher conversions than the previously mentioned sulfate catalysts under the same reaction conditions (0.76 M—70% conversion, 1.52 M—67% and 0.076 M—60%). Each catalyst displayed very similar reaction profiles with an induction period lasting no longer than 30 min, followed by a steady decline in acetylene conversion for the remaining reaction time resulting in conversions of $\approx 50\%$. Altering the concentration therefore only had a small effect on the initial conversion and a negligible effect on the residual conversion at 240 min. XPS analysis of each fresh catalyst using S 2p and O 1s scans (Table S2, Supporting Information) showed very similar atomic concentrations of sulfur (0.4–0.6 at%) and oxygen (77–9.4 at%). These values explain the very similar acetylene

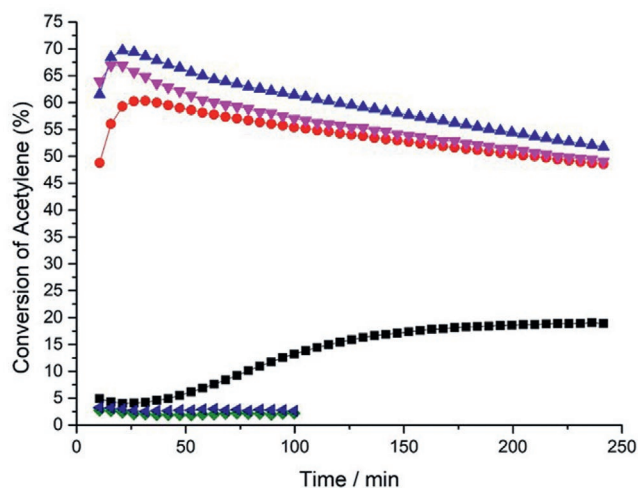


Figure 4. H_2SO_4 pre-wash catalysts time-on-line data—Au/C-AR (■), 0.076 M H_2SO_4 (●), 0.76 M H_2SO_4 (▲), 1.52 M H_2SO_4 (▼), 0.76 M H_2SO_4 carbon (◆), and carbon (◄).

conversions, despite the use of varied concentrations of acid. Each freshly prepared catalyst also showed mixtures of Au(0), Au(I), and Au(III), however, no quantification of the proportions of gold species could be performed due to the reducing nature of the XPS beam which could lead to erroneous values.^[27] XRD analysis (Figure S5a, Supporting Information) confirmed that none of the fresh catalysts contained gold nanoparticles (only fresh 0.076 M pre-wash catalyst shown for clarity, both fresh 0.76 and 1.52 M appeared identical to this), whilst the used catalysts showed only small reflections owing to nanoparticle formation, visible at $38^\circ/2\theta$. This indicates that in addition to the high activity, the supported gold remained relatively stable throughout the reaction with the majority remaining as atomically dispersed gold and not sintering at high acetylene conversion (although small clusters would remain undetectable via XRD). This is dissimilar to previously reported high activity Au/C catalysts which display significant growth of gold nanoparticles,^[30] suggesting that the atomically dispersed gold is less mobile on those catalysts pre-washed with H_2SO_4 . Further characterization was performed on the most active, 0.76 M pre-wash, catalyst to determine whether the small proportion of gold nanoparticle formation as observed in the used catalyst occurred due to heating or under reaction conditions. Analysis of in situ XRD patterns of the catalyst heated under nitrogen (Figure S5b, Supporting Information) demonstrated that, $<240^\circ\text{C}$, no reflections corresponding to gold nanoparticles were observed. Above this temperature, characteristic reflections at 38° , 44° , 65° , and $78^\circ/2\theta$ became visible. Therefore, the small nanoparticles observed in the used catalyst (Figure S5a, Supporting Information) were formed due to the reaction gases introduced at 200°C . The sintering of gold observed at 240°C indicates that the gold was less stable than in Au/C-AR, which began sintering at 320°C (Figure S5c, Supporting Information). Therefore, doping the carbon support with sulfur has reduced the stability of the catalyst at higher temperatures than those typically used in the acetylene hydrochlorination reaction.

XPS analysis was performed on the 0.76 M pre-wash catalyst, after it had been heated to 200°C under argon gas and then allowed to cool (heated), after reaching maximum initial conversion (used, max. conversion), and after 240 min reaction (used, 240 min) and compared to Au/C-AR (Table S3, Supporting Information). The 0.76 M pre-wash catalysts showed

little variation the concentrations of surface sulfur (0.3–0.5 at%) and oxygen (6.6–8.8 at%). As expected, the sulfur values were higher in the all pre-wash catalysts than Au/C-AR (0.1 at%), whilst the concentration of O (7.6%) was comparable in both fresh pre-wash and Au/C-AR. From these results it can be concluded that the sulfur treatment only adds a small relative fraction of sulfur to the pre-wash catalyst, however this is still sufficient to have a remarkable enhancement in catalytic activity, albeit with a slight loss of stability. The majority of the sulfur introduced to the catalyst remains after reaction, as only a loss of 0.2 at% occurs, whilst the concentration of oxygen also remains constant.

Following the promising activity at 200°C , further tests were performed on samples of the 0.76 M pre-wash catalysts at lower temperatures (Figure S6a, Supporting Information). A reaction was initiated at 100°C and the temperature increased in 25°C increments until 175°C . The catalyst was inactive from 100 to 150°C , however, light-off occurred at 175°C . Further tests carried out between 150 and 175°C determined that the catalyst had a high rate of change of conversion at 160°C and above (Figure S6b, Supporting Information). This light-off showed that the 0.76 M pre-wash catalyst was active at temperatures below that of Au/C-AR and with a relatively short induction period compared to Au/C-AR, both desirable qualities for industrial application. The test performed at 155°C showed the acetylene conversion steadily increased over the catalyst as a function of reaction time, however, the test was stopped before reaching a steady conversion. This temperature was determined to be the lowest at which the catalyst was active under these reaction conditions.

XANES analysis was performed to compare the gold oxidation state of the fresh 0.76 M pre-wash catalyst and those tested at 160 and 200°C . These were also compared to Au/C-AR and gold foil for reference (Figure 5a). Fresh 0.76 M pre-wash catalyst was composed of a mix of Au(I) and Au(III) states, with more Au(III) character present than observed in fresh Au/C-AR. After reaction, the used 0.76 M pre-wash catalyst tested at 160°C was very similar to the fresh sample, with only a modest loss of Au(III) concentration. Increasing the temperature to 200°C caused a further reduction, resulting in an increased Au(I) concentration, very similar to that of Au/C-AR. The acetylene conversion over Au/C-AR and the 0.76 M pre-wash at

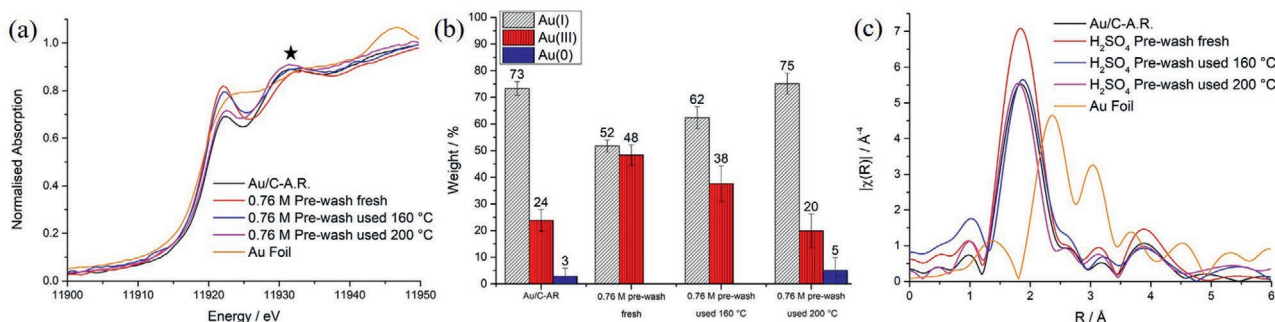


Figure 5. a) Au L_3 -edge XANES of Au/C-AR, pre-wash 0.76 M H_2SO_4 fresh, used at 160°C , and used at 200°C and Au foil reference. ★ symbol shows position of second prominent scattering feature >11930 eV. b) Linear combination fitting of the Au L_3 -edge XANES for the fresh aqua regia catalyst, fresh and used at 160°C , and 200°C 0.76 M H_2SO_4 pre-wash catalysts. c) Fourier transform of the k^3 -weighted χ EXAFS data of Au/C-AR, pre-wash 0.76 M H_2SO_4 fresh, used at 160°C , and used at 200°C and Au foil reference.

200 °C, differed by 34% despite the comparable oxidation states ratios. This suggests that another factor must contribute to the activity of the catalyst, such as dispersion of gold, availability of active sites, or the interaction of the gold with reactants. LCF of the XANES data was performed to quantify the fraction of the gold oxidation states present in each catalyst (Figure 5b). This data showed a mix of Au(I)—52% and Au(III)—48% in the fresh 0.76 m pre-wash sample. Following treatment under reaction conditions, the percentage of Au(I) increased, to 62% in the used 0.76 m pre-wash 160 °C and 75% in the used 0.76 m pre-wash 200 °C samples, matched by a corresponding decrease in Au(III). The used 0.76 m pre-wash 200 °C sample also had a small increase in Au(0) content (5%). This data does not correspond well with the XANES white line heights shown in Figure 5a, which can be explained by the fitting of the standards to the reference materials (Figure S7a–d, Supporting Information). In all the EXAFS analysis performed so far it was assumed that oxidized gold existed as gold chloride, due to the HAuCl_4 precursor and the abundance of chlorine in the solvent, aqua regia. However, upon introduction of sulfur to the carbon support, the XANES data for the 0.76 m pre-wash catalysts no longer fit well with the Au–Cl references, hence the XANES absorption values not agreeing with the LCF data. In the four figures shown (Figure S7a–d, Supporting Information) it is important to note that a smaller *R*-Factor and Chi-square value indicates a better data fit, as the maximum value of uncertainty of the fit is equal to 1.^[31,32] Using Au/C-AR as an example of “good fit” values (*R*-factor 0.000914, Chi-square 0.01377), the values of the 0.76 m pre-wash used 160 °C sample and 0.76 m pre-wash used 200 °C sample are both over 1.5 times the *R*-factor and chi-square values. This does not however explain the disparity between fresh 0.76 m pre-wash (*R*-factor 0.000723, Chi-square 0.01043) and Au/C-AR.

It was reported that Au(I)-S and Au–Cl can be differentiated by the ligand affected scattering feature, Au(I)-S at 11 930 eV and Au–Cl having two shifts due to the different oxidation states; lower energy, 11 923 eV, with Au(I)-Cl and higher energy, 11 934 eV, with Au(III)-Cl.^[33] An Au–S standard was not run during the XANES analysis shown in Figure 5a to compare against. However the Au(I) and Au(III) chloride standards both show a shift in energy from 11 931 to 11 936 eV, respectively (Figure S2, Supporting Information). Comparing the fresh and used 0.76 m pre-wash catalysts scattering feature around the same energy range (★ in Figure 5a), shows a decreasing trend in energy for each catalyst, as noted in Table S4, Supporting Information. This implies that fresh 0.76 m pre-wash was composed of Au–S, with a scattering energy of 11 933 eV, between those of Au(I) and Au(III). Performing the reaction at 160 °C resulted in a shift in scattering energy to 11 932 eV and increasing the temperature to 200 °C resulted in a further shift to 11 931 eV, the same as that of Au(I). Therefore, subjecting the catalyst to reaction gases and increasing the temperature may have resulted in a change of Au speciation, from more Au–S to Au–Cl, or perhaps a mix of both. Further tests would be needed using appropriate Au–S standards and preferably an in situ reaction to determine if this was the case.

The EXAFS appears to show that all of the fresh and used 0.76 m pre-wash catalysts are composed of Au–Cl (Figure 5c). Unfortunately, the scattering patterns of sulfur and chlorine

appear virtually indistinguishable via EXAFS due to their atomic number differing by only one.^[27,33,34] Therefore, the results shown in Figure 5c for the fresh and used 0.76 m pre-wash catalysts only show a sharp scattering path at 1.8 Å, identified as the interaction of Au with a lighter element, in this case chlorine or sulfur. These results do show a much higher intensity of oxidized gold in the fresh 0.76 m pre-wash sample than that for Au/C-AR, perhaps owing to the higher concentration of S. However, after reaction at 160 and 200 °C the intensity of the scattering was the same as that of Au/C-AR, suggesting a loss of this new species. This same trend was observed in Au/C- CoSO_4 (Figure 2c) albeit with a much higher initial intensity of Au–Cl/Au–S ratio, therefore, it is reasonable to suggest that the decrease in Au–Cl/Au–S intensity occurred during heating. No scattering associated with Au–Au was observed. As EXAFS is a global averaging technique, the small presence of nanoparticles detected by XRD in Figure S5a, Supporting Information may not have been observed here due to the abundance of oxidized gold present.

High angle annular dark field scanning transmission electron microscopy (HAADF-STEM) was performed on the 0.76 m H_2SO_4 prewash fresh and used catalysts to further elucidate whether Au remained as atomically dispersed species (Figure 6a–e). As expected, the fresh catalyst contained only atomically dispersed Au species (Figure 6a,b). The sample used at 160 °C also contains atomically dispersed Au, however clusters are also present (Figure 6c,d). The sample used at 200 °C contained atomically dispersed Au along with clusters (Figure 6e) as seen in the 160 °C sample. Crucially, however, field emission gun scanning electron microscope (FEG-SEM) images at low magnification (Figure 6f) also revealed large Au particles and “wires” in the sample used at 200 °C, that would not have been observed by HAADF-STEM. These results confirm the lower stability of this catalyst at 200 °C, with the deactivation observed resulting from formation of nanoparticles and loss of atomically dispersed Au species. The catalyst appears to be more stable at 160 °C, with no deactivation observed over the time studied. However, the presence of clusters, as observed by HAADF-STEM and XRD suggesting the presence of small amounts of nanoparticles, confirms that this treatment does not form fully stable catalysts, despite the promising high activity.

Four further 0.76 m H_2SO_4 prewash supports were prepared by variation of the amount of water used in the washing step (previous 100 mL) to determine the effect of this step on the final activity of the catalysts. Volumes of 0, 50, 500, and 1000 mL were used to wash the carbon, after which a 1 wt% Au/C catalyst was prepared on the dried carbon. These were compared to Au/C-AR and 0.76 m pre-wash prepared using 100 mL H_2O , as shown previously and in Figure 7a. Using high volumes of H_2O , 1000 and 500 mL, resulted in a small decrease in maximum initial conversion (58% and 55%, respectively) compared to 100 mL (70%). This would be expected as a higher volume of water would result in the removal of more sulfur from the support, thereby removing anchoring points for gold. This could lead to a decrease in dispersion of gold cations, reducing the activity of the catalyst. Alternatively, the lower amount of sulfur on the surface may reduce any benefit in reactant adsorption due to sulfur containing compounds, as described in the literature,^[25] thereby resulting in a lower relative activity. The

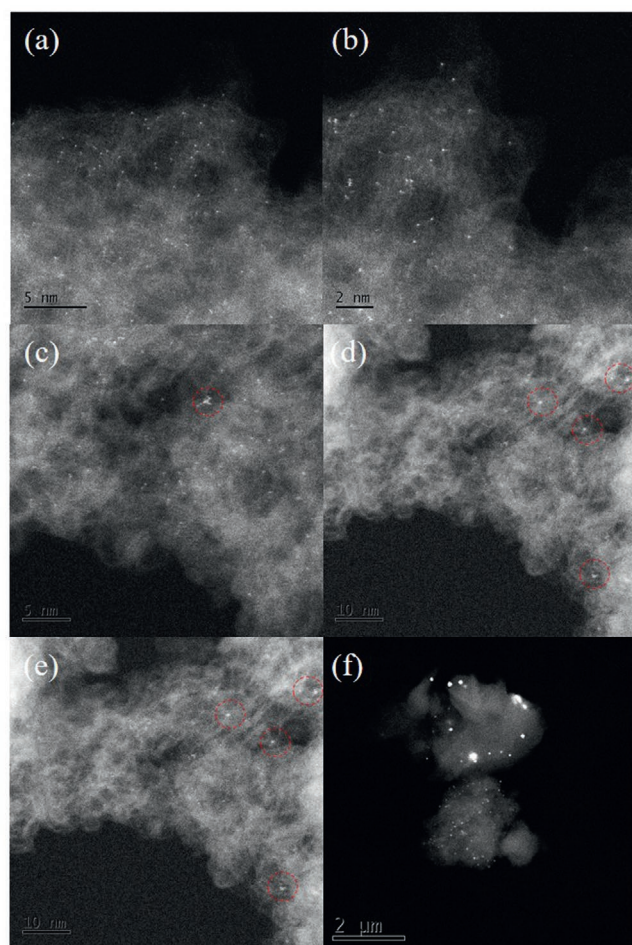


Figure 6. HAADF-STEM images of pre-wash 0.76 M H_2SO_4 a,b) fresh, c,d) used at 160 °C, and e) used at 200 °C. f) FEG-SEM image of pre-wash 0.76 M H_2SO_4 used at 200 °C.

catalyst washed with 50 mL of H_2O initially achieved an acetylene conversion comparable to the catalyst that underwent a wash volume of 1000 mL (58%), but this decreased at a greater rate, resulting in a catalyst which had a lower final conversion (42%, compared to 48%). This catalyst may have contained

more acid on the support, hence the more rapid onset of deactivation. This was observed in the catalyst which was not washed with H_2O (0 mL) which showed a rapid deactivation, followed by a stable, low conversion of 5%. Acid sites are a known cause of Au/C catalyst deactivation, due to acid catalyzed acetylene polymerization which coats the surface of the catalyst, blocking the active sites and rendering the catalyst inactive.^[2,30]

Analysis of microwave plasma atomic emission spectroscopy (MP-AES) spectra from the filtrate of these carbons was performed to determine the mass of sulfur removed from the supports during the washing process. The results (Figure 7b) show that the mass of sulfur removed increases significantly with increasing wash volume from 50 to 100 mL (234 and 304 mg, respectively). However, after increasing the volume to 500 and 1000 mL there is only a small increase in mass of sulfur removed, from 332 to 372 mg, respectively. These results show that the catalyst washed with 50 mL of H_2O removed 1.3 times less sulfur than that washed with 100 mL. One could suggest therefore that a much greater mass of sulfur remained on the catalyst, which may explain the more rapid deactivation of the 50 mL washed catalyst. Using volumes of water greater than 100 mL had little effect on the mass of sulfur removed from the catalyst, hence the similar reaction profiles observed in Figure 7a.

These MP-AES results fit well with XPS analysis performed on the same catalysts. Table S5, Supporting Information shows that the catalyst washed with 50 mL H_2O contains the highest concentration of sulfur (0.8 at%), whilst the catalysts washed with 100, 500, and 1000 mL of H_2O had very similar atomic concentrations (0.5–0.6 at%). The change in oxygen concentrations did not match those of sulfur, likely due to the high concentration of oxygen present in the Au/C-AR catalyst and the presence of multiple non-sulfur containing oxygen functionalities (Table S3, Supporting Information—7.6%).

2.3.2. Post Treatment of Au/C Catalyst with Sulfuric Acid

A series of post-wash H_2SO_4 Au/C catalysts were also prepared to determine if the observed enhancement was sensitive to order of preparation. As with pre-wash H_2SO_4 catalysts, three initial concentrations of acid were chosen; 0.076, 0.76, and 1.52 M. However, unlike the pre-wash catalysts, varying the

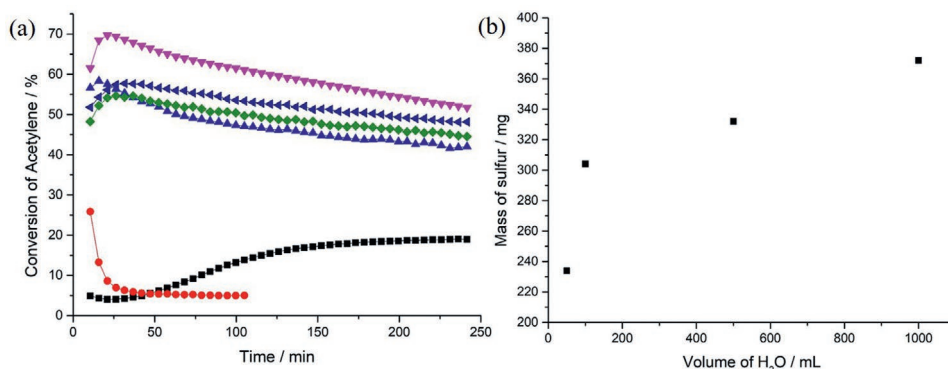


Figure 7. a) Acid pre-wash catalysts with varying volumes of H_2O wash time-on-line data—Au/C-AR (■), 0 mL wash (●), 50 mL wash (▲), 100 mL wash (▼), 500 mL wash (◆), and 1000 mL wash (◀). b) Mass of sulfur removed from 0.76 M H_2SO_4 pre-wash catalyst as determined by MP-AES versus volume of water used to wash catalyst.

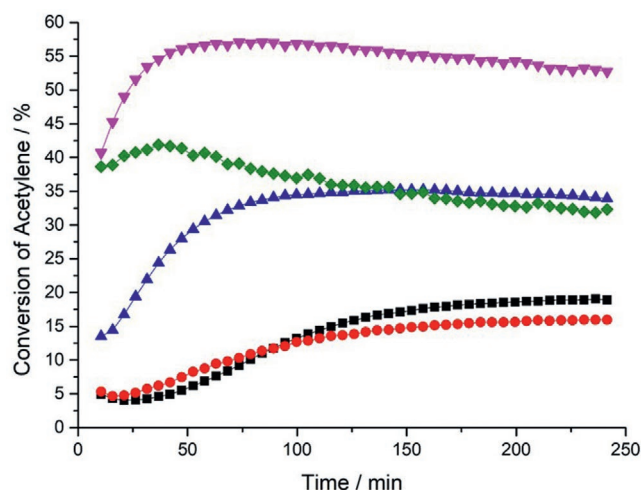


Figure 8. H_2SO_4 post-wash catalysts time-on-line data—Au/C-AR (■), 0.076 M H_2SO_4 (●), 0.76 M H_2SO_4 (▲), 1.52 M H_2SO_4 (▼), and 7.6 M H_2SO_4 (◆).

concentration of H_2SO_4 in the post-wash resulted in significant changes in catalytic activity (Figure 8). The acetylene conversion over the 0.076 M post-wash catalyst was comparable to that of Au/C-AR, with slightly lower final conversion (16% and 19%, respectively). Increasing the concentration to 0.76 M resulted in an increase in conversion (35%), followed by a stable conversion for the remaining reaction time. Post-treatment with 1.52 M increased the initial conversion further, to 57%, however this was then followed by a slow deactivation, as was observed for all the pre-wash H_2SO_4 catalysts. As the conversion increased with H_2SO_4 concentration, a higher concentration was used (7.6 M) to determine if this trend would continue. Due to the high acidity of 7.6 M H_2SO_4 , this catalyst was centrifuged after stirring in acid to separate the solvent from the solid catalyst, then 100 mL of H_2O added and centrifuged again, and finally dried. This method was used as the filter paper was readily dissolved in the concentrated acid. Figure 8 illustrates that such a high concentration of acid resulted in a rapid deactivation compared to that over the other post-wash catalysts. This deactivation could be ascribed to the introduction of more acid sites with this high concentration of acid, which would catalyze the polymerization of VCM, again blocking the active gold species.^[35] However, XPS showed little variation in the sulfur and oxygen atomic concentrations (Table S6, Supporting Information) and no changes in mass balance were detected, therefore deactivation may be via another mechanism such as Au agglomeration.

XRD analysis revealed that the 0.076 M post-wash sample contained nanoparticles before and after reaction (Figure S8, Supporting Information). This is likely due to the dilute acid and low oxidizing ability of the solvent, as shown in Figure S3b, Supporting Information, which led to a mobilization of the gold and formation of nanoparticles. However, the activity profile shown in Figure 8 confirms that seemingly enough oxidized gold was stabilized on the support to produce an active catalyst. The reaction also did not result in nanoparticle growth, confirming the stability of the 0.076 M post-wash catalyst.

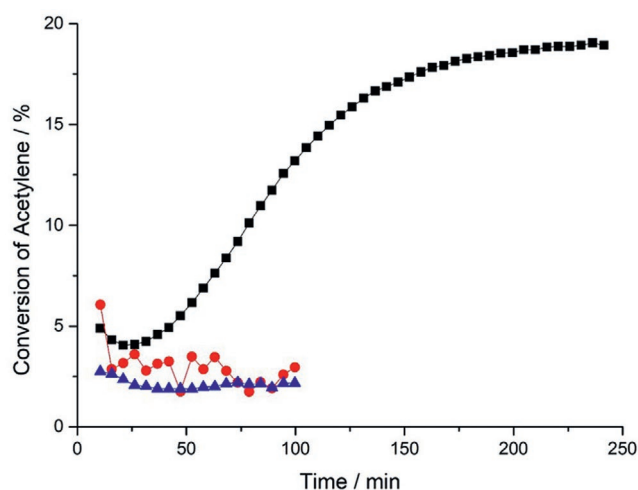


Figure 9. H_2SO_4 catalysts time-on-line data—Au/C-AR (■), Au/C-0.76 M H_2SO_4 solvent (●), and Carbon-0.76 M H_2SO_4 (▲).

Analysis of the 0.76 M post-wash catalyst did not contain any nanoparticles prior to the reaction, however, they were present in the used catalyst. Over the 1.52 M post-wash catalyst the reaction profile was comparable to that over the pre-wash catalysts (Figure 4) and similarly lacked nanoparticles before and after reaction, demonstrating this catalyst was able to maintain a high concentration of oxidized gold during high acetylene conversion.

Nanoparticles were observed in the fresh and used 7.6 M post-wash samples at approximately in the same order as those of 0.076 M, however both catalysts display very different activity profiles. The 7.6 M post-wash catalyst has an initial high conversion which was thought to deactivate due to the high number of acid sites which would facilitate acetylene polymerization, as opposed to the agglomeration of gold (Table S6, Supporting Information).^[2,30] These results show that varying the concentration of H_2SO_4 in post-wash catalysts had a much more significant effect on the catalytic activity than the pre-wash.

2.3.3. Other Sulfuric Acid Treatments

Two more variations in the preparation of H_2SO_4 catalysts were introduced to confirm the role of sulfur in the preparation. First, a catalyst was prepared using 0.76 M H_2SO_4 as a solvent for HAuCl_4 (Au/C-0.76 M H_2SO_4 solvent). This was to determine whether H_2SO_4 had the oxidizing ability to prepare a monodispersed gold on carbon without the aid of aqua regia. Second the carbon pre-wash support (C-0.76 M H_2SO_4) was tested without gold, to ensure that gold was necessary for the catalyst to be active.

Figure 9 shows that both materials had low conversions. For Au/C-0.76 M H_2SO_4 solvent, the low conversion was ascribed to the presence of large gold nanoparticles (>50 nm, calculated via the Scherrer equation) as determined by XRD analysis (Figure S9, Supporting Information), present before reaction which grew upon introduction to reaction conditions. It has been shown previously that the use of water as a solvent for the preparation of Au/C catalysts results in poor activity, owing to the inability of water to maintain gold in an oxidized form.^[27]

This dilute acid would behave in a similar manner, hence the low acetylene conversion. C-0.76 M H_2SO_4 displayed a low conversion as there was no gold present.

3. Conclusion

In this work Au/C carbon catalysts were doped with sulfur using a range of sulfur containing compounds and by a number of methods to produce highly active catalysts for the acetylene hydrochlorination reaction. Although bimetallic catalysts prepared with chloroauric acid and metal sulfates were found to be active, eliminating the second metal suggested that sulfur was the crucial species for the activity enhancement. Catalyst activity was found to be sensitive to the identity of the cation in the sulfate precursor and, also the order of preparation. Pre-washing carbon in sulfuric acid resulted in catalysts with a high initial activity which decreased slowly over a 4 h reaction period. XPS showed that a marginal increase in sulfur concentration, compared to Au/C-AR (0.1 to 0.5 at%), had a large effect on the conversion whilst XRD and XAFS confirmed that the catalyst was still predominately comprised of monodispersed cationic gold before and after reaction. This dispersion was consistent with previous data on Au/C-AR, however the high catalytic activity may be the result of a slight change in oxidation state toward an initially greater proportion of Au(III). EXAFS also indicated the presence of another interaction other than Au–Cl, most likely to be that of Au–S species, although further analysis using appropriate standards would be needed to confirm this. Significantly, changing the concentration of acid in the pre-wash had little effect on the acetylene conversion, with the volume of water used for washing being the main determining factor. Alternative methods of treating the catalyst, such as using a post-wash, resulted in catalysts with a poorer performance than the pre-wash, however, these were largely still more active than Au/C-AR, albeit with seemingly lower stability. These results demonstrate the promising use of sulfur as a promoter for the gold catalyzed hydrochlorination of acetylene.

4. Experimental Section

Preparation of Standard 1% Au/C: Chloroauric acid (20 mg) was dissolved in aqua regia (3 HCl: 1 HNO_3), or other solvents (eg. H_2SO_4 , water) as stated, (2.7 mL) and allowed to stir for 10 min. The metal precursor solution was added drop wise, with stirring to ground, activated, dry carbon (0.99 g). This solution was left to stir for 1 h then dried under nitrogen at 140 °C for 16 h.

Preparation of Pre-Treated Carbon: To prepare pre-treated carbons, the following method was used, using pre-prepared sulfate solutions (5 g of metal sulfate in 15 mL of H_2O); ammonium sulfate, sodium sulfate or pre-prepared equimolar acids; sulfuric acid, hydrochloric acid, nitric acid, phosphoric acid, and aqua regia. In all cases, the sulfates and acids were dissolved and diluted in deionized water to form equimolar solutions, with the exception of aqua regia. When an equimolar solution was not used, this was stated in the text.

15 mL of the prepared solution was stirred on 1.15 g of activated carbon for 1 h. The solution was filtered under vacuum, washed with deionized water (100 mL) and dried at 110 °C for 16 h. All catalysts were prepared to a 1 wt% Au loading on carbon.

Preparation of Post Treated Carbons: To prepare post-wash catalysts, a 1% Au/C catalyst was first prepared. This catalyst (1.15 g) was then stirred in a

pre-prepared solution (15 mL) for 1 h, the solution filtered under vacuum, washed with deionized water (100 mL) and dried at 110 °C for 16 h.

Reaction Conditions for Acetylene Hydrochlorination: Unless otherwise stated, all reactions were conducted using the following conditions. C_2H_2 : HCl 1:1.02, balanced in argon, total gas flow 50 mL min^{-1} , catalyst (0.09 g), 200 °C, ambient pressure. Analysis of the acetylene hydrochlorination reaction was carried out using a Varian CP-3800 GC fitted with a Poropak-N packed column and an FID detector. Conversion of acetylene was calculated using Equation (1).

$$\text{Acetylene conversion (\%)} = \frac{\text{Initial acetylene peak area} - \text{Final acetylene peak area}}{\text{Initial acetylene peak area}} \times 100 \quad (1)$$

Powder X-Ray Diffraction: Analysis was performed between 10° and 80° 2 θ using an X'Pert Pro PAN Analytical powder diffractometer employing a Cu $K\alpha$ radiation source operating at 40 keV and 40 mA. Analysis of the spectra obtained was carried out using X'Pert High Score Plus software.

In Situ Powder X-Ray Diffraction: In situ powder XRD analysis was performed using an X'pert Pro XRD fitted with an Anton-Parr XRK900 in situ cell between 20° and 80° 2 θ at different temperatures, whilst heating under a nitrogen flow, 50 mL min^{-1} . Analysis of the spectra obtained was carried out using X'Pert High Score Plus software.

X-Ray Photoelectron Spectroscopy: Analysis was performed on a Thermo Fisher Scientific K-alpha⁺ spectrometer. Samples were analyzed using a micro-focused monochromatic Al X-ray source (72 W) over an area of ≈ 400 microns. Data were recorded at pass energies of 150 eV for survey scans and 40 eV for high resolution scan with 1 and 0.1 eV step sizes, respectively. Charge neutralization of the sample was achieved using a combination of both low energy electrons and argon ions. Data analysis was performed in CasaXPS using a Shirley type background and Scofield cross sections, with an energy dependence of -0.6 .

Microwave Plasma Atomic Emission Spectroscopy: Analysis was performed using an Agilent 4100 MP-AES. Liquid samples from each catalyst washing were collected and analyzed against calibration solutions from analytical standards.

Microscopy: Microscopy was performed using a Tescan MAIA3 FEG-SEM operating at 15 kV. Images were acquired using the backscattered electron detector. Samples were dispersed as a powder onto 300 mesh copper grids coated with Holey carbon film. HAADF-STEM data were acquired using a JEOL ARM200CF microscope in the electron Physical Science Imaging Centre in Diamond. The instrument was operated at 200 kV. Powdered catalyst samples were dry dispersed onto lacy carbon films over a 400 mesh copper grid

Supporting Information

Supporting Information is available from the Wiley Online Library or from the author.

Acknowledgements

The authors would like to thank Johnson Matthey for funding. The authors would also like to thank Diamond Light Source (DLS) and electron Physical Science Imaging Centre (ePSIC) for their support and access to the Aberration Corrected Microscope (Instrument E01 session number MG23498-5). The authors would also like to thank DLS for access to the B18 beamline for XAS studies (allocation numbers SP15214, SP15151-7 and SP15151-9). SP and GJH would like to thank the Max Planck Centre on the Fundamentals of Heterogeneous Catalysis (FUNCAT) for funding.

Conflict of Interest

The authors declare no conflict of interest.

Data Availability Statement

All the information is in the manuscript or the supplementary data.

Keywords

acetylene, gold, hydrochlorination, sulfur, VCM

Received: November 16, 2020

Revised: December 19, 2020

Published online: February 25, 2021

- [1] United Nations Environment Programme, Minamata Convention on Mercury, www.mercuryconvention.org (accessed: September 2020).
- [2] P. Johnston, N. Carthey, G. J. Hutchings, *J. Am. Chem. Soc.* **2015**, 137, 14548.
- [3] H. Zhang, B. Dai, X. Wang, W. Li, Y. Han, J. Gu, J. Zhang, *Green Chem.* **2013**, 15, 829.
- [4] H. Zhang, W. Li, X. Li, W. Zhao, J. Gu, X. Qi, Y. Dong, B. Dai, J. Zhang, *Catal. Sci. Technol.* **2015**, 5, 1870.
- [5] J. Zhao, J. Xu, J. Xu, J. Ni, T. Zhang, X. Xu, X. Li, *ChemPlusChem* **2015**, 80, 196.
- [6] Y. Pu, J. Zhang, X. Wang, H. Zhang, L. Yu, Y. Dong, W. Li, *Catal. Sci. Technol.* **2014**, 4, 4426.
- [7] J. Zhao, S. Gu, X. Xu, T. Zhang, X. Di, Z. Pan, X. Li, *RSC Adv.* **2015**, 5, 101427.
- [8] H. Zhang, B. Dai, W. Li, X. Wang, J. Zhang, M. Zhu, J. Gu, *J. Catal.* **2014**, 316, 141.
- [9] Y. Dong, H. Zhang, W. Li, M. Sun, C. Guo, J. Zhang, *J. Ind. Eng. Chem.* **2016**, 35, 177.
- [10] C. Huang, M. Zhu, L. Kang, X. Li, B. Dai, *Chem. Eng. J.* **2014**, 242, 69.
- [11] J. Zhang, Z. He, W. Li, Y. Han, *RSC Adv.* **2012**, 2, 4814.
- [12] C. J. Davies, P. J. Miedziak, G. L. Brett, G. J. Hutchings, *Chin. J. Catal.* **2016**, 37, 1600.
- [13] M. Conte, A. F. Carley, G. Attard, A. A. Herzing, C. J. Kiely, G. J. Hutchings, *J. Catal.* **2008**, 257, 190.
- [14] J. Zhao, Y. Yu, X. Xu, S. Di, B. Wang, H. Xu, J. Ni, L. L. Guo, Z. Pan, X. Li, *Appl. Catal., B* **2017**, 206, 175.
- [15] H. Zhang, B. Dai, X. Wang, L. Xu, M. Zhu, *J. Ind. Eng. Chem.* **2012**, 18, 49.
- [16] S. Wang, B. Shen, Q. Song, *Catal. Lett.* **2010**, 134, 102.
- [17] M. Zhu, Q. Wang, K. Chen, Y. Wang, C. Huang, H. Dai, F. Yu, L. Kang, B. Dai, *ACS Catal.* **2015**, 5, 5306.
- [18] C. Hagelüken, in *Handbook Of Heterogeneous Catalysis*, Wiley-VCH Verlag GmbH & Co. KGaA, Weinheim, Germany **2008**, pp. 1846–1863.
- [19] C. Zhang, H. Zhang, Y. Li, L. Xu, J. Li, L. Li, M. Cai, J. Zhang, *ChemCatChem* **2019**, 11, 3441.
- [20] X. Li, X. Pan, X. Bao, *J. Energy Chem.* **2014**, 23, 131.
- [21] X. Li, Y. Wang, L. Kang, M. Zhu, B. Dai, *J. Catal.* **2014**, 311, 288.
- [22] K. Zhou, B. Li, Q. Zhang, J. Q. Huang, G. L. Tian, J. C. Jia, M. Q. Zhao, G. H. Luo, D. S. Su, F. Wei, *ChemSusChem* **2014**, 7, 723.
- [23] J. Wang, F. Zhao, C. Zhang, L. Kang, M. Zhu, *Appl. Catal., A* **2018**, 549, 68.
- [24] X. X. Di, J. Zhao, Y. Yu, X. L. Xu, S. C. Gu, H. H. He, T. T. Zhang, X. N. Li, *Chin. Chem. Lett.* **2016**, 27, 1567.
- [25] X. Qi, W. Chen, J. Zhang, *RSC Adv.* **2019**, 9, 21931.
- [26] X. Duan, L. Ning, Y. Yin, Y. Huang, J. Gao, H. Lin, K. Tan, H. Fang, L. Ye, X. Lu, Y. Yuan, *ACS Appl. Mater. Interfaces* **2019**, 11, 11317.
- [27] G. Malta, S. A. Kondrat, S. J. Freakley, C. J. Davies, L. Lu, S. Dawson, A. Thetford, E. K. Gibson, D. J. Morgan, W. Jones, P. P. Wells, P. Johnston, C. R. A. Catlow, C. J. Kiely, G. J. Hutchings, *Science* **2017**, 355, 1399.
- [28] G. Malta, S. A. Kondrat, S. J. Freakley, D. J. Morgan, E. K. Gibson, P. P. Wells, M. Aramini, D. Gianolio, P. B. J. Thompson, P. Johnston, G. J. Hutchings, *Chem. Sci.* **2020**, 11, 7040.
- [29] X. Liu, M. Conte, D. Elias, L. Lu, D. J. Morgan, S. J. Freakley, P. Johnston, C. J. Kiely, G. J. Hutchings, *Catal. Sci. Technol.* **2016**, 6, 5144.
- [30] G. Malta, S. A. Kondrat, S. J. Freakley, C. J. Davies, S. Dawson, X. Liu, L. Lu, K. Dymkowski, F. Fernandez-Alonso, S. Mukhopadhyay, E. K. Gibson, P. P. Wells, S. F. Parker, C. J. Kiely, G. J. Hutchings, *ACS Catal.* **2018**, 8, 8493.
- [31] C. H. Booth, Y. J. Hu, *J. Phys.: Conf. Ser.* **2009**, 190, 012028.
- [32] B. Ravel, Athena XAS Data Processing, <http://Brukeravel.Github.io/Demeter/Documents/Athena/Examples/Aucl.html> (Accessed: June 2017).
- [33] Z. Song, J. P. L. Kenney, J. B. Fein, B. A. Bunker, *Geochim. Cosmochim. Acta* **2012**, 86, 103.
- [34] M. F. Lengke, B. Ravel, M. E. Fleet, G. Wanger, R. A. Gordon, G. Southam, *Environ. Sci. Technol.* **2006**, 40, 6304.
- [35] B. Nkosi, N. J. Coville, G. J. Hutchings, M. D. Adams, J. Friedl, F. E. Wagner, *J. Catal.* **1991**, 128, 366.